

Precipitation-generated oscillations in open cellular cloud fields

Graham Feingold¹, Ilan Koren², Hailong Wang³, Huiwen Xue⁴ & Wm. Alan Brewer¹

Cloud fields adopt many different patterns that can have a profound effect on the amount of sunlight reflected back to space, with important implications for the Earth's climate. These cloud patterns can be observed in satellite images of the Earth and often exhibit distinct cell-like structures associated with organized convection at scales of tens of kilometres^{1–3}. Recent evidence has shown that atmospheric aerosol particles—through their influence on precipitation formation—help to determine whether cloud fields take on closed (more reflective) or open (less reflective) cellular patterns^{4,5}. The physical mechanisms controlling the formation and evolution of these cells, however, are still poorly understood⁶, limiting our ability to simulate realistically the effects of clouds on global reflectance. Here we use satellite imagery and numerical models to show how precipitating clouds produce an open cellular cloud pattern that oscillates between different, weakly stable states. The oscillations are a result of precipitation causing downward motion and outflow from clouds that were previously positively buoyant. The evaporating precipitation drives air down to the Earth's surface, where it diverges and collides with the outflows of neighbouring precipitating cells. These colliding outflows form surface convergence zones and new cloud formation. In turn, the newly formed clouds produce precipitation and new colliding outflow patterns that are displaced from the previous ones. As successive cycles of this kind unfold, convergence zones alternate with divergence zones and new cloud patterns emerge to replace old ones. The result is an oscillating, self-organized system with a characteristic cell size and precipitation frequency.

For over a century, phenomena related to Rayleigh–Bénard⁷ convection have fascinated both the scientific community and the casual observer of natural systems. Cellular and roll-like patterns can be seen in a host of phenomena, and at many scales, ranging from boiling water on the kitchen stove to magmatic convection in the Earth's mantle. Our interest is in the vast sheets of low clouds on the west coasts of continents that exhibit myriad, sometimes intricate, planforms, which often manifest Rayleigh–Bénard convection in the form of cellular convection at the mesoscale (a few to several hundred kilometres)^{1–3}. These clouds are important because they increase the reflectance of shortwave radiation and therefore exert a cooling effect on the climate system that is not compensated by appreciable changes in outgoing longwave radiation⁸.

Laboratory experiments have shown that Rayleigh–Bénard cells emerge as a result of convection between two horizontal surfaces separated by a sufficiently large temperature gradient. To transfer heat most effectively, the system self-organizes into various patterns such as rolls, hexagonal or cellular structures. The relevant non-dimensional number is the Rayleigh number⁷ $Ra = \alpha g \Delta T h^3 / (\nu \chi)$, where ΔT is the temperature difference between surfaces, α is the thermal expansion coefficient, g is gravitational acceleration, h is the

separation between the surfaces, ν is the kinematic viscosity, and χ is the thermal diffusivity. Theory shows that convection develops when Ra exceeds a critical value Ra_c ($\approx 10^3$).

Although fundamental buoyant processes are common to both mesoscale cellular convection and classical Rayleigh–Bénard convection, the latter cannot explain certain characteristics of atmospheric convection. For example, there is a disparity in the aspect ratio of cells ($\sim 20:1$ for mesoscale cellular convection versus $\sim 3:1$ for Rayleigh–Bénard convection) due to factors such as latent heating associated with phase changes and large-scale dynamics^{2,9,10}. In atmospheric convection an effective Rayleigh number is derived by replacing ν and χ with their eddy counterparts so that the effective $Ra \approx 10^5$ for $h = 1$ km (ref. 10).

For $Ra > Ra_c$, Rayleigh–Bénard theory shows that the system can select a range of characteristic length scales; this suggests that the structure and dimensions of the topology may evolve in time and space¹¹. Exactly how a given system selects a particular subset of permitted parameter space has been the subject of much investigation. Evolution to an optimal spatial scale can be inhibited by what are termed contraselective factors¹¹, one of which is the interaction between adjacent convective cells. The interacting cells can be viewed as elastic entities competing for space within the system. The relevance to cloud systems will soon become apparent.

In accordance with theory, cloud systems driven by cooling at the upper boundary prefer a closed cellular structure (broader, buoyant updraught regions surrounded by narrower and stronger negatively buoyant downdraughts); whereas those driven by surface heating favour open cells (strong, narrow updraughts surrounding broader, weaker downdraughts)¹². Thus asymmetry in the vertical heating (cooling) profile selects the appropriate asymmetry in the horizontal cellular structure¹³.

A number of new studies, however, are pointing to the role of precipitation in selecting the cloud pattern^{4–6,14}. Evaporative cooling associated with rain falling below cloud provides additional asymmetry in the cooling profile and has been shown to select the open rather than the closed cellular state, all else being equal^{15–17}.

To explore the role of precipitation in transforming open cellular cloud patterns we simulated cloud systems exhibiting open and closed cellular states using large eddy simulation (Fig. 1). The model solves the Navier–Stokes equations and simulates aerosol effects on cloud microphysical processes¹⁷ (see Supplementary Information). Distinct patterns of closed and open cells, closely mimicking satellite observations, can be seen in the synthetic cloud albedo fields. The simulations differ only in their initial aerosol concentrations: high aerosol concentrations result in closed cells (non- or weakly precipitating clouds) and low concentrations in open cells (precipitating clouds). The very fact that the aerosol has the potential to control cloud albedo and equilibrium cellular state is noteworthy¹⁸.

¹NOAA Earth System Research Laboratory (ESRL), Chemical Sciences Division, Boulder, Colorado 80305, USA. ²Department of Environmental Sciences, Weizmann Institute, Rehovot 76100, Israel. ³Pacific Northwest National Laboratory, Richland, Washington 99352, USA. ⁴Department of Atmospheric Sciences, School of Physics, Peking University, 5 Yiheyuan Road, Beijing 100871, China.

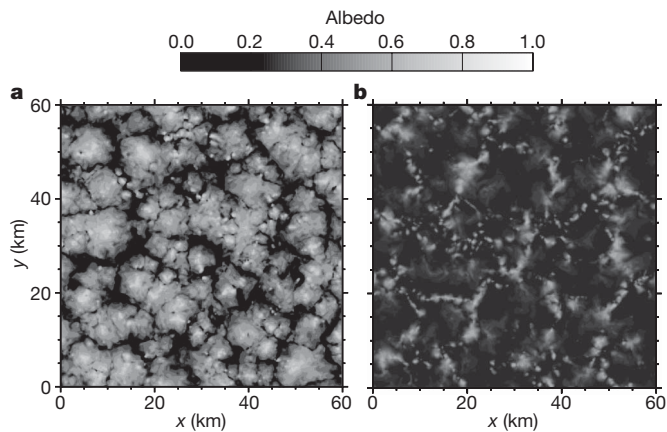


Figure 1 | Cloud albedo calculated from large eddy simulation of closed and open cellular structures. The simulations differ only in the magnitude of the initial aerosol concentrations. High aerosol concentrations favour non-precipitating closed cells (a) while low aerosol concentrations favour precipitating open cells (b). The brightest regions are associated with the thickest clouds and (in the case of open cells) the precipitation-generating zones.

The existence of precipitation provides a new and relatively unexplored perturbation to the open cellular convective system. In the simulations thick clouds are generated in the strong updraughts associated with the cell walls. The Y-shaped convergence zones where adjacent cells connect are sites where convergence and new updraughts, and therefore the potential for precipitation, is greatest^{16,17,19}. With

time the precipitation generated by these thick clouds falls below the cloud base, evaporating and cooling the air during its descent. The cool downward current has a vertical motion of opposite sign to that in the cloud that spawned the precipitation. The result is a negative feedback on the system that forces divergence in the very locations that a short while ago were regions of peak convergence. The existing cell structure is disrupted and new open cells are born (Fig. 2a–c and Supplementary Fig. 1). We refer to this as an oscillating cellular convective system. The coupled oscillators^{20–22} are the individual precipitating regions, each of which drives downdraughts, cold pools and surface divergence. The coupling occurs when outflows from adjacent cells collide and form surface convergent zones that result in updraughts. These updraughts in turn generate thick clouds and eventually precipitation, thus repeating the cycle. This evolution manifests as a spatially varying pattern of clouds and precipitation. Remarkably, satellite imagery, corrected for advection by the mean wind so that spatial patterns in successive images can be compared, also shows bright regions, associated with cloud walls, replaced by dark, cloud-free regions, only to be replaced again by bright clouds (Supplementary Figs 3 and 4). Ship-based lidar and radar (light and radio detection and ranging) observations from a recent field campaign²³ augment the satellite view and provide compelling evidence for the divergence/convergence processes associated with precipitation-driven outflows that generate the oscillations (Fig. 2d and Supplementary Information).

To clarify how precipitation disrupts steady-state cellular convection and perpetuates its own self-organizing patterns, we use a model²⁴ that solves the Navier–Stokes equations in two dimensions, but with the addition of a simplified version of the precipitation feedback. The effects of precipitation are simulated by applying a

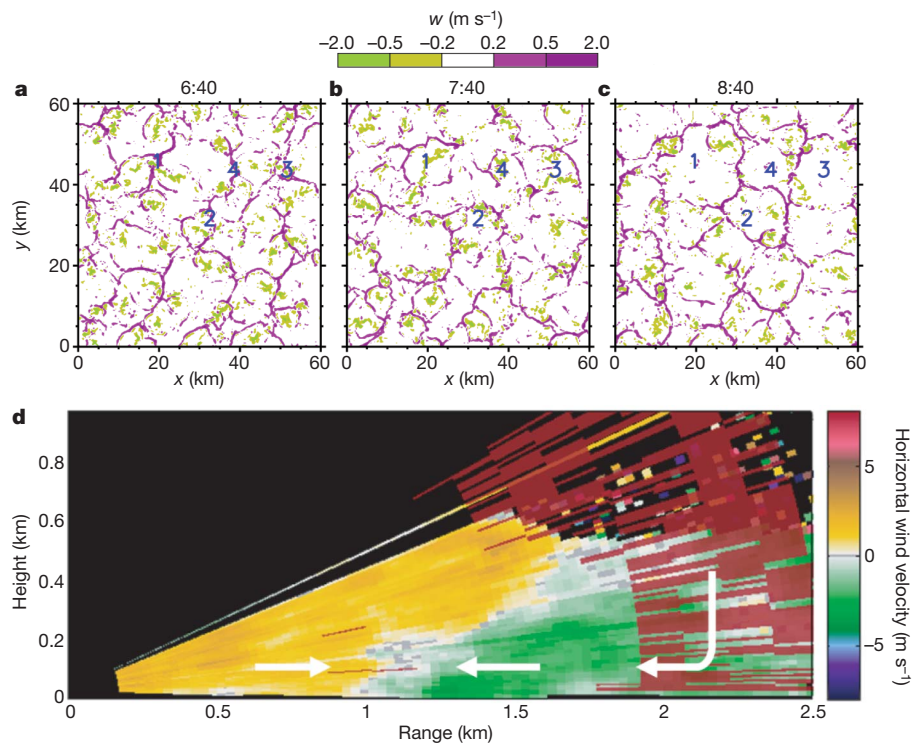


Figure 2 | Updraught and downdraught patterns illustrating surface convergence and divergence zones in open cells. a–c, Plan views of near-surface updraught (purple) and downdraught (green) patterns, each separated by one hour. w is vertical velocity; positive values are updraughts and negative values are downdraughts. Updraught regions correspond to surface convergence, and downdraughts to surface divergence zones. Four Y-shaped updraught patterns in a are labelled 1, 2, 3 and 4 to illustrate the evolution of the open cellular structures from one time (times relative to the start of the simulation) to the next (6:40 to 7:40 to 8:40). They occur at strong convergence zones and are favoured for the strongest convection. As time

progresses (b and c), precipitation at these points changes the surface flow to a divergent one. New cellular structures emerge from the old planform as the cold-pool outflows interact with one another and generate new convergence zones that in turn generate new precipitation zones. d, Vertical cross-section of a precipitation-generated outflow and creation of a convergence zone as observed by ship-based radar and Doppler lidar (located at range 0 km and height 0 km). Radar reflectivity (>20 dB Z; dark red) is indicative of significant rain. Lidar data show air flow towards (green) and away from (yellow) the lidar. Arrows indicate the direction of flow.

time-varying, negatively buoyant force to any strong, positively buoyant cell for a period of time that mimics the duration of a precipitation event. Thus if a rising parcel becomes too buoyant (that is, produces thick cloud and the potential for rain), it suffers a penalty and experiences a commensurate negative buoyancy for a finite period of time, much like the system shown in Fig. 2. In Fig. 3 we demonstrate how a system evolves from a conductive system to a static oscillating convective system comprising fixed couplets of updraughts and downdraughts (normalized time τ between 100 and 300). The Rayleigh–Bénard system can either maintain its structure when exposed to weaker simulated precipitation perturbations ($300 < \tau < 600$), or oscillate between states as a result of stronger precipitation events ($600 < \tau < 800$). (See Supplementary Information for details.)

Time-series analysis of large-eddy-simulation-derived surface precipitation rate substantiates the claim that the system represents a coupled oscillator comprising interacting precipitating cells (Fig. 4). The three time series in Fig. 4a derive from two different numerical models applied to three different atmospheric soundings, each yielding cells of different sizes. All time series exhibit distinct periodicity in precipitation of the order of a half-hour to one-and-a-half hours, with larger cell sizes associated with longer periodicity. The oscillations are further demonstrated by contours of rain rate that show a ‘gridded’ structure of rain with distinct spatial/temporal periodicity. The precipitating cells communicate with neighbouring cells and synchronize the onset of rain, as demonstrated in Supplementary Fig. 2. There is also evidence that similar processes occur in deep convective systems that exhibit self-organization^{22,25}.

Self-organizing properties are evident in a host of natural systems ranging from fundamental physics (for example, laser emission of coherent light), to the life sciences (the fluid, organized movement of a flock of birds), the Earth sciences (as in the cellular cloud example above), and free-market economies²⁶. The fundamental principle of self-organization is that a system-wide order emerges from local interactions or competition between system components, as exemplified in Figs 1 and 2, and identified as contraselective factors in Rayleigh–Bénard theory¹¹. In the present case the local interaction occurs between surface divergent flows associated with adjacent precipitating cells. The novel part of this work is that the precipitation generation and dissipation causes rearrangements between different open-cell

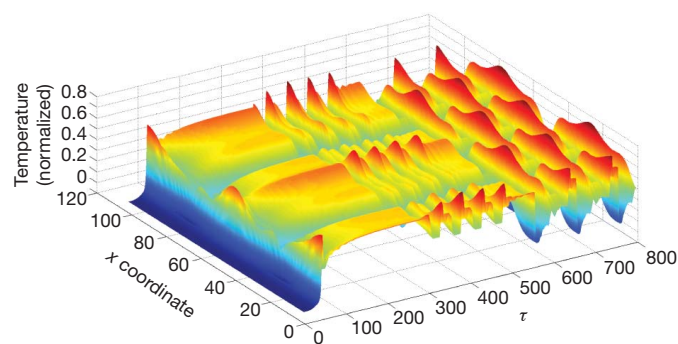


Figure 3 | A simple two-dimensional model of Rayleigh–Bénard convection and oscillating Rayleigh–Bénard convection. Results are at normalized height $z = 0.5$ ($0 \leq z \leq 1$) and for normalized time τ . The colour scheme is a rendering of the normalized temperature. The period $0 < \tau < 100$ shows the transition from conduction to convection. The period $100 < \tau < 300$ shows a steady-state convective pattern developing. The period $300 < \tau < 600$ shows relatively small negative temperature perturbations, of one-quarter of the temperature gradient, applied to the locations of maximum temperature for a period of one-quarter of the relaxation time of the system. The system is resilient to the perturbations. The period $600 < \tau < 800$ shows larger temperature perturbations of one-third of the temperature gradient applied for a period of one-third of the relaxation time. The system oscillates back and forth between steady states as the simulated effects of precipitation modify the open cellular structure.

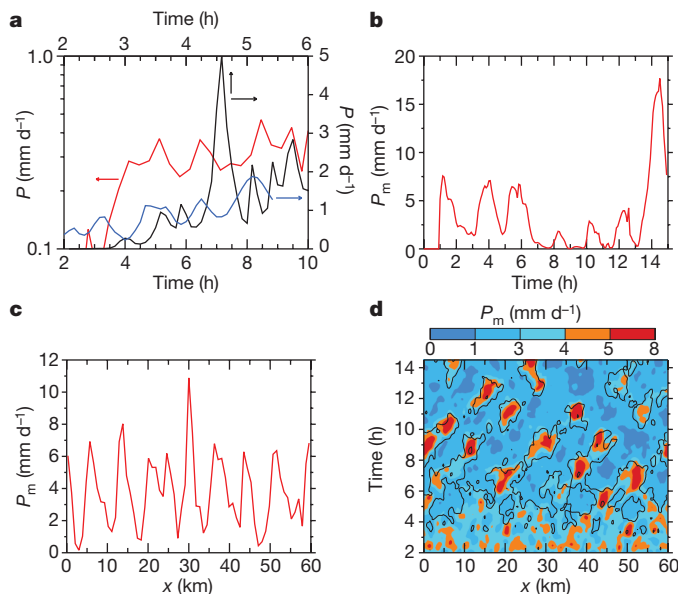


Figure 4 | Oscillations in precipitation rate. **a**, Time series of domain-averaged surface precipitation rate P associated with simulations in Fig. 2 (cell size ~ 15 km; red line), P from an Atlantic Ocean sounding with smaller cell size (~ 4 km; black line¹⁶) and P from a southeast Pacific Ocean sounding with larger cell size (~ 20 km; blue line)³⁰. We note the distinct periodicity in surface P and the relationship between cell size and precipitation frequency. **b**, Time series of column-maximum precipitation P_m for a subset of the Fig. 2 domain, further illustrating oscillatory behaviour. **c**, P_m as a function of x (horizontal) distance over a limited range of y (horizontal) distance at a single model time step. **d**, Contours of P_m in x –time space showing a ‘gridded’ structure of P_m with distinct spatial/temporal periodicity. (That is, combinations of **b** and **c**, but with averaging over the entire y distance.) The column-maximum vertical velocity (solid contours; averaged over all y as in P_m) is well-correlated with P_m . Precipitation in cloud systems that are not organized exhibits time series characterized by intermittent, irregular events.

states, creating a level of organization that has to our knowledge not been previously shown.

A characteristic of self-organizing systems is that they are robust^{26,27}. Notwithstanding the oscillations between different open-cell states (Figs 2 and 3), the system is resilient in the sense that the open cells do not disappear, or convert to a closed cellular state. A break in an open-cell cloud wall means that adjacent cells metamorphose, distort and expand into the ‘uncontested’ space (as in Fig. 2). The coupling between existing cells is sufficient to overcome complete disruption in the order, and provided that the precipitation does not cease through a significant part of the domain, the order remains intact. The analogy to networks is also noteworthy: if poorly connected nodes (interacting cells) are damaged then the system will repair itself, whereas if strongly connected nodes are damaged the self-organization will disappear²⁸.

As a further comment on the robustness of these states we consider the fact that not all precipitating stratocumulus clouds generate open cells⁵ even though precipitation may be locally as strong as that observed in open-cell conditions. The closed-cell state is also robust and self-repairing. Our modelling suggests that it is only when precipitation becomes sufficiently strong and widespread that local outflows can interact with one another, compete for space and make the transition to the open cellular state. Indeed, it has been shown that the rate of growth of the open cells depends on the rain rate in individual cells, as well as the spatial distribution of rain¹⁷.

In summary, precipitation adds two interesting elements to mesoscale cellular convection. First, it provides an additional source of asymmetry in the cooling profile that contributes to the selection of the open-cellular state^{15–17}. Second, it creates a hitherto undocumented case of cellular convection that rearranges between different open planforms. As old precipitation zones dissipate, new ones are

generated through local interaction between cells. The precipitation is synchronized and therefore characterized by periodic behaviour. Robustness, a characteristic of self-organized systems and networks, is demonstrated by resilience to the various perturbations experienced by the system²⁶. Finally, we note that aerosol particles are known to suppress precipitation in warm clouds, and therefore indirectly play a pivotal role in controlling marine boundary layer cloud and its morphological structure, with potentially important consequences for the Earth's radiation balance^{18,29}.

METHODS SUMMARY

Four major analysis tools are brought to bear on the problem. (1) Large eddy simulation of the cloud system that includes coupled solution to the Navier–Stokes equations, and aerosol–cloud–precipitation–radiation interactions to demonstrate the oscillating open-cellular system. The model domain size is 60 km × 60 km × 1.5 km. The grid size is 300 m horizontally and 30 m vertically and the time step is 3 s. (2) A two-dimensional Navier–Stokes model, solved using a lattice Boltzmann method, is used to elucidate the fundamental principles of transition from conduction-dominated to convection-dominated heat transfer, steady-state solution to Rayleigh–Bénard convection, and the effect of negative buoyancy forcing associated with precipitation in generating an oscillating open-cellular system. (3) Meteosat geostationary satellite imagery is used to illustrate how an open cell shifts from one state to another by first removing the effects of the mean advective wind. (4) Ship-based lidar and radar remote sensing data taken in a precipitating open-cellular cloud field during the VOCALS-REx field programme²³ in the southeast Pacific Ocean (<http://www.eol.ucar.edu/projects/vocals/>) is applied to document convergence and divergence patterns associated with precipitation outflows. The lidar is a 2- μm Doppler system with radial wind velocity accuracy of the order of 0.2 m s⁻¹. The radar is the NOAA C-band (5.4 cm) precipitation radar.

Received 22 February; accepted 22 June 2010.

- Krueger, A. F. & Fritz, S. Cellular cloud patterns revealed by TIROS I. *Tellus* **13**, 1–7 (1961).
- Agee, E. M. Observations from space and thermal convection: a historical perspective. *Bull. Am. Meteorol. Soc.* **65**, 938–949 (1984).
- Garay, M. J. & Davies, R. Averill, C. & Westphal, J. A. Actiniform clouds: overlooked examples of cloud self-organization at the mesoscale. *Bull. Am. Meteorol. Soc.* **85**, 1585–1594 (2004).
- Stevens, B. *et al.* Pockets of open cells and drizzle in marine stratocumulus. *Bull. Am. Meteorol. Soc.* **86**, 51–57 (2005).
- Sharon, T. M. *et al.* Aerosol and cloud microphysical characteristics of rifts and gradients in maritime stratocumulus clouds. *J. Atmos. Sci.* **63**, 983–997 (2006).
- Wood, R. *et al.* Open cellular structure in marine stratocumulus sheets. *J. Geophys. Res.* **113**, doi:10.1029/2007JD009371 (2008).
- Rayleigh, L. On convection currents in a horizontal layer of fluid, when the higher temperature is on the under side. *Phil. Mag.* **32**, 529–546 (1916).
- Twomey, S. The influence of pollution on the shortwave albedo of clouds. *J. Atmos. Sci.* **34**, 1149–1152 (1977).
- Atkinson, B. W. & Zhang, J.-W. Mesoscale shallow convection in the atmosphere. *Rev. Geophys.* **34**, 403–431 (1996).
- Krishnamurti, R. On cellular cloud patterns—Part 1: Mathematical model. *J. Atmos. Sci.* **32**, 1353–1363 (1975).
- Getling, A. V. *Rayleigh–Bénard Convection: Structures and Dynamics*. In *Advanced Series in Nonlinear Dynamics* Vol. 11 (World Scientific, 2001).
- Graham, A. Shear patterns in an unstable layer of air. *Phil. Trans. R. Soc.* **A232**, 285–296 (1933).
- Helfand, M. & Kalnay, E. A mechanism for open or closed cellular convection. *J. Atmos. Sci.* **40**, 631–650 (1983).
- Rosenfeld, D., Kaufman, Y. J. & Koren, I. Switching cloud cover and dynamical regimes from open to closed Benard cells in response to the suppression of precipitation by aerosols. *Atmos. Chem. Phys.* **6**, 2503–2511 (2006).
- Savic-Jovcic, V. & Stevens, B. The structure and mesoscale organization of precipitating stratocumulus. *J. Atmos. Sci.* **65**, 1587–1605 (2008).
- Xue, H., Feingold, G. & Stevens, B. Aerosol effects on clouds, precipitation, and the organization of shallow cumulus convection. *J. Atmos. Sci.* **65**, 392–406 (2008).
- Wang, H. & Feingold, G. Modeling mesoscale cellular structures and drizzle in marine stratocumulus. Part I: Impact of drizzle on the formation and evolution of open cells. *J. Atmos. Sci.* **66**, 3237–3256 (2009).
- Baker, M. & Charlson, R. J. Bistability of CCN concentrations and thermodynamics in the cloud-topped boundary layer. *Nature* **345**, 142–145 (1990).
- Willis, G. E. & Deardorff, J. W. Laboratory observations of turbulent penetrative-convection plumes. *J. Geophys. Res.* **84**, 295–302 (1979).
- Strogatz, S. H. Exploring complex networks. *Nature* **410**, 268–276 (2001).
- Arenas, A. *et al.* Synchronization in complex networks. *Phys. Rep.* **469**, 93–153 (2008).
- Yair, Y., Aviv, R. & Ravid, G. Clustering and synchronization of lightning flashes in adjacent thunderstorm cells from lightning location networks data. *J. Geophys. Res.* **114**, D09210, doi:10.1029/2008JD010738 (2009).
- Wood, R. *et al.* Preliminary confrontation of the VOCALS hypotheses with observations and modeling. *CLIVAR* **7**, 5–9 (2009).
- Guo, Z., Shi, B. & Zheng, C. A coupled lattice BGK model for the Boussinesq equations. *Int. J. Numer. Methods Fluids* **39**, 325–342 (2002).
- Parodi, A., Emmanuel, K. A. & Provenzale, A. Plume patterns in radiative convective flow. *New J. Phys.* **5**, 106.1–106.17 (2003).
- Heylighen, F. The science of self-organization and adaptivity. In *Encyclopedia of Life Support Systems* (EOLSS, 2001).
- Wang, H. & Feingold, G. Modeling mesoscale cellular structures and drizzle in marine stratocumulus. Part II: The microphysics and dynamics of the boundary region between open and closed cells. *J. Atmos. Sci.* **66**, 3257–3275 (2009).
- Barabási, A.-L. & Albert, R. Emergence of scaling in random networks. *Science* **286**, 509–512 (1999).
- Albrecht, B. A. Aerosols, cloud microphysics and fractional cloudiness. *Science* **245**, 1227–1230 (1989).
- Wang, H., Feingold, G., Wood, R. & Kazil, J. Modelling microphysical and meteorological controls on precipitation and cloud cellular structures in southeast Pacific stratocumulus. *Atmos. Chem. Phys. Discuss.* **10**, 6347–6362 (2010).

Supplementary Information is linked to the online version of the paper at www.nature.com/nature.

Acknowledgements We thank NOAA's Climate Goal Program, a CIRES Visiting Fellowship (I.K.) and the Pacific Northwest National Laboratory (H.W.) for supporting this work. We acknowledge the www.LBMethod.org project for sharing the Lattice Boltzmann Method theory and code, and S. C. Tucker and S. E. Yuter for their support in acquiring the lidar and radar data during the VOCALS-REx field experiment. C. A. Ennis provided editorial assistance and D. Fisher helped with the figures.

Author Contributions The principal idea was conceived jointly by G.F. and I.K. The large eddy simulations were designed and performed by H.W., H. X. and G.F. I.K. performed the two-dimensional model simulations and the satellite image analysis. W.A.B. performed the analysis of the lidar data. All authors discussed the results and commented on the manuscript.

Author Information Reprints and permissions information is available at www.nature.com/reprints. The authors declare no competing financial interests. Readers are welcome to comment on the online version of this article at www.nature.com/nature. Correspondence and requests for materials should be addressed to G.F. (graham.feingold@noaa.gov).